Tuijin Jishu/Journal of Propulsion Technology
ISSN: 1001-4055
Vol. 44 No. 2 (2023)

Energy and Exergy Analysis of a Rectangular-Shaped Mini-Channel Flat-Plate Solar Collector Using Tio_2-Water and Cu-Water Nanofluids

Abhay Kumar Singh[1*], Suresh Kant Verma[2]

[1]Department of Mechanical Engineering, National Institute of Technology Patna, Patna, 80005, India*
[2]Department of Mechanical Engineering, National Institute of Technology Patna, Patna, 80005, India
Co-author Email Id: [2]skverma@nitp.ac.in

Corresponding Author: Abhay Kumar Singh[1*]
[1]Department of Mechanical Engineering, National Institute of Technology Patna, Patna, 80005, India*
Email Id: [1]kumarabhay347@gmail.com*

Abstract: Flat plate solar collectors (FPSC) are commonly used for a variety of applications and have a very simple design. However, the main drawbacks of the collector are its low outlet temperature and poor thermal performance. In present study, the fluid outlet temperature, heat removal factor, energy efficiency, exergy efficiency, and pressure drop have been evaluated for a rectangular-shaped minichannel FPSC operating with two different nanofluids (Cu-water and TiO_2-water). The ranges of volumetric concentration ratio and mass flow rate are 1-5% and 0.01-0.07kg/s, respectively. A mathematical model based on the energy balance has been solved using energy equation solver software. The result revealed that fluid outlet temperature, mean plate temperature, and overall heat loss coefficient (HLC) increase with increasing concentration ratios for both nanofluids. But at the same concentration ratio and MFR, the fluid outlet temperature, mean plate temperature, and overall HLC for Cu-water nanofluid are greater than those of TiO_2-water. The outlet temperature and mean plate temperature for the nanofluid TiO_2-water of volumetric ratio 1% are 369.4K and 347.9 K, respectively, and these values increase to 395.9K and 351.1K at volumetric ratio 5% for the same MFR of 0.01 kg/s. Efficiency and heat removal factor for the TiO_2-water nanofluid are greater than those for the Cu-water nanofluid for the same MFR and concentration ratio. Pressure drop increases with increasing concentration ratios for both fluids, but it is greater for Cu-water as compared to TiO_2-water.

Keywords: *Flat plate, solar collector, mini-channel, Nanofluid, thermal performance.*

1. Introduction

The modularization and industrialization of the world have drastically increased the demand for energy in recent decades. The high demand for energy burdens conventional resources of energy, which are in very limited amounts on the earth, and affects people economically due to their high price and environmentally due to their ability to pollute the environment. Recently, the price of petroleum has reached such a high level that people are motivated to search for new sources of energy that can be used as substitutes for conventional resources of energy. These energy sources could include solar, wind, tidal, ocean, or ocean energy. One of the cleanest and most widely accessible non-conventional energy sources on the planet is solar energy (Raj & Subudhi, 2018)

Solar energy can be converted into thermal energy by means of a device known as a solar collector. One collector that operates at low to medium temperatures and has a simple design is the flat plate solar collector (FPSC). This collector's low efficiency and low outlet temperature are its key issues.

2. Literature survey

2.1. Literature survey based FPSC using nanofluid

Many studies have used various active and passive techniques to improve the performance of PFSC (Murugan et al., 2022).The effectiveness of heat transfer can be increased by increasing the thermal conductivity of heat transfer fluid (Javadi, Saidur, & Kamalisarvestani, 2013) (Muhammad et al., 2016). According to a review study, a small quantity of nanoparticles added to the base fluid can improve the efficiency and performance of solar collectors (Sami, Kazi, & Badarudin, 2015). The effect of nanoparticle size on Al_2O_3-water nanofluid was observed by Said et al. (2016) in an experimental study, and it was reported that 13 nm Al_2O_3 nanofluid was more efficient than that of 20 nm Al_2O_3 (Said, Saidur, & Rahim, 2016). When CuO-water nanofluid with a particle size of 40 nm was utilised, Moghadam et al. (2014) found that the thermal efficiency of FPSC was raised by 21.8% at a mass flow rate(MFR) of 1 kg/min (Jabari, Farzane-gord, Sajadi, & Hoseyn-zadeh, 2014).TiO_2-water was utilised by Said et al. (2015) as a heat transfer fluid for FPSC and they found that with a volume fraction of 0.1% and a MFR of 0.5 kg/min,the energy efficiency and exergy efficiency increased by 76.6% and16.9%,respectively(Said, Sabiha, Saidur, Hepbasli, Rahim, Mekhilef, et al., 2015). He et al.(2014) carried out an experimental investigation into the impact of Cu-water nanofluid taking into account the various mass fraction and size of nanoparticles and they come to the conclusion that for the 25nm particle size and mass mass fraction of 0.2%, FPSC efficiency was raised by 23.83% (He, Zeng, & Wang, 2015). Based on a review study (Sami et al., 2015)(Zayed, Zhao, Du, Kabeel, & Shalaby, 2019)(Alawi et al., 2021), it is concluded that carbon-bead nanofluid is the most efficient for the solar collector as its very low concentration enables it to enhance the performance of FPSC. The effect of using graphene nanofluid on the heat transfer performance of FPSC and various challenges associated with graphene nanofluid have been discussed by (Sadeghinezhad et al., 2016). Heat transfer is found to be boosted by 21% when nanofluid with a 0.5% volume concentration is employed, and heat transfer increases even further up to 49.75% when twisted tape with a twist ratio of 5 is incorporated into the solar collector (Sundar, Singh, Punnaiah, & Sousa, 2017). Sint et al. (2017) reported in their theoretical study that up to 2% volume concentration of CuO-water nanofluid increased the efficiency of FPSC by 5% (Khin, Sint, Choudhury, Masjuki, & Aoyama, 2017). Sundar et al. (2018) used longitudinal strip inserts and Al2O3 nanofluid for investigating the performance of FPSC. They found that employing 0.3% volumetric concentration boosted the thermal effectiveness of the collector to 58%, and adding a longitudinal strip with aspect ratio 1 at a Reynolds number of 13500 increased it to 84% (Sundar, Kirubeil, Punnaiah, Singh, & Sousa, 2018). The efficiency of FPSC is boosted by 10.74% at a reduced temperature of zero when CeO_2-water nanofluid is used with a volume fraction of 0.066% and a mass flux of 0.019 kg/sm^2 (Sharafeldin & Gróf, 2018).

The transient behavior of FPSC using Al_2O_3-water nanofluid was investigated for the determination of thermal inertia of FPSC components and it was reported that the outlet temperature of the collector increased by 7.2 % for 3% volumetric concentration of Al_2O_3-water nanofluid and 0.004 kg/s mass flow rate in July month while in October maximum thermal efficiency of 83.9 % was achieved at 0.06 kg/s mass flow rate and 1 % volume concentration of Al2O3-water nanofluid (Mete, Akif, & Turgut, 2018). Kilic et al. (2018) concluded based on an experimental study that the instantaneous efficiency of FPSC increases from 36.2% to 48.67% when 2% (wt) of TiO_2-water nanofluid is used as heat transfer fluid Dobriyal et al(2019) tried to summarize different performance improvement techniques of FPSC which reduce the losses to surrounding and allow to maximize the absorption of solar radiation (Dobriyal, Negi, Sengar, & Singh, 2019). The efficiency of the collector enhances from 52% to 58% when 0.3% Cu-water nanofluid is included, and it grows even more up to 64% when a twisted tape with a twist ratio of 5 is introduced inside the tube, with a maximum friction penalty of 1.477 times as compared to plain FPSC (Sundar, Misganaw, Singh, & Sousa, 2020). Moravej et al. (2020) reported that the maximum efficiency of FPSC could be achieved up to 78% by using 1 wt% of TiO_2-water nanofluid (Moravej, Vahabzadeh, Guan, & Li, 2020). In their experimental study, Sundar et al. (2021) used Cu-water nanofluid at volume concentrations of 1% and 3% to investigate the transfer of heat, friction factor, and instantaneous thermal efficiency of FPSC Sundar, Punnaiah, Singh, Pereira, & Sousa, 2021). In order to increase convection heat transfer and reduce heat losses accumulated near the contact region, a FPSC equipped with a revolutionary tube and magnetic field inducer was designed by Bezaaatpour and Rostamzadeh (2021). They reported that the hybrid system with Fe_2O_3-water nanofluid enabled an increase in efficiency from 44.4% to 61.7% (Bezaatpour & Rostamzadeh, 2021). The efficiency of FPSC is enhanced by 2.48% and 8.46% by using 0.5% Al_2O_3 and 0.5% crystal nanocellulose, respectively (Farhana et al.,

2021). (Akram et al., 2021) investigated the effect of using carbon and metal oxide-based nanofluids for FPSC, and they revealed that the thermal efficiency of the collector was enhanced by 17.45%, 13.05%, and 12.36% for 0.1 wt% of each carbon nanoplatelet, ZnO, and SiO_2, respectively. The energetic and exergetic performance of CuO-water nanofluid was reported to be better as compared to Al_2O_3-water (Allouhi & Amine, 2021). Some recent developments, techniques, and challenges associated with FPSC and photovoltaic systems using nanofluid are summarised by (Sheikholeslami, Ali, Ebrahimpour, & Said, 2021). Nanofluid by dispersing a composite of silica and titanium in an equal ratio was used by (Abu-hamdeh, Alazwari, Salilih, Sajadi, & Karimipour, 2021) for investigating the performance of FPSC. A numerical method was applied for the analysis of the performance of FPSC integrated with turbulence inducer and SWCNT-CuO/water hybrid nanofluid, and it was found that hybrid nanofluid enables the increase of the thermal performance of FPSC at lower concentrations (Nabi, Pourfallah, Gholinia, & Jahanian, 2022) Energy efficiency and the rise in environmental pollutants are investigated for FPSC using Cu-Al/water hybrid nanofluids (Mustafa, Alqaed, & Sharifpur, 2022). The thermal performance of FPSC integrated with a vortex genrator insert and TiO_2-water nanofluid was investigated by (Bagher, Saedodin, Hadi, Doostmohammadi, & Khaledi, 2022) and it was concluded that at the optimal volume flow rate, thermal losses decreased by 42.46% and optical efficiency increased by 14.5%.

2.2. Literature survey based on minichannel FPSC

Using the minichannel inside the absorber plate is another passive technique to enhance the performance of solar collector has been reported by various researchers (Vahidinia & Khorasanizadeh, 2021). (Sharma & Diaz, 2011) investigated numerically the performance of minichannel based solar collector and made comparison to the evacuated tube collector. (Mansour, 2013) revealed that heat removal factor (HRF) of FPSC with minichannel is 16.1 % higher than that of the Conventional collector. Aluminum based minichannel FPSC has been designed and compared to the Conventional FPSC of copper material and it is observed that minichannel based solar collector 13 % more efficient than the conventional for same operating condition (Robles, Duong, Martin, Guadarrama, & Diaz, 2014). Thermo-hydraulic performance of micro-channel FPSC was investigated by (Oyinlola, Shire, & Moss, 2015). Absorber plate with rectangular channel and plate with U-bend serpentine tube, two different configuration of absorber plate were analyzed on the basis of thermo-hydraulic performance of collector. It was revealed that plate with rectangular channel was 18 % more efficient than that of surpentne-tube. But at higher range of temperature, the overall efficiency of plate with serpentine-tube collector was 9 % higher than that of rectangular channel collector(Arvanitis, Papanicolaou, Mathioulakis, Belessiotis, & Bouris, 2020). Particle swarms optimization method was used for optimizing the different operating parameters of a minichannel FPSC (Mohan, Dinesha, & Iyengar, 2021). Thermo-physical performance of large size minichannel FPSC and small size minichannel FPSC were evaluated and compared with conventional FPSC at same operating conditions. It was found that thermal performance of large size and small size minichannel FPSC were comparable and better than conventional one but hydraulic performance of size minichannel collector are better than that of small size(Vahidinia & Khorasanizadeh, 2021).

3. Scope and work Contributions

The literature explores the application of various passive approaches for enhancing FPSC performance. Numerous researches assess the performance of the collector in conventional FPSC that employs a variety of metal and nonmetal nanofluids as heat transfer fluids. To improve the performance of the collector, several researchers have experimented with different absorber plate configurations, such as a rectangular channel, a plate with a serpentine tube, or a plate with a minichannel.

- However, further investigation is needed to evaluate the performance of MFPSC with the implementation of nanofluids
- To the authors' knowledge and based on prior research, no previous studies using nanofluids in a rectangular-shaped minichannel FPSC have been reported.
- For MFPSC, energy and exergy analysis utilising nanofluids is required.

4. Problem explanation

In this present study, a MFPSC of dimensions (2.8 m x 1.4 m x 0.1 m) has been proposed as shown in Fig.1. A 4 mm thick aluminium plate is used as an absorber plate. Twenty minichannels of width 40mm and depth 2mm are created on the aluminium plate. The distance between two consecutive minichannels is 30mm. The other specifications of considered MFPSC are illustrated in table 1. Two different nanofluids (Cu-water and TiO_2-water) have been used as heat transfer fluids inside the rectangular channel. The properties of nanoparticles are given in table.2. Thermo-hydraulic performance of the MFPSC has been measured for both nanofluids and compared with each other for different MFRs, water inlet temperatures, and concentration ratios. The metrological conditions for this study are shown in Table.3. This study comprises:

- Analysis of the fluid outlet temperature, mean plate temperature (MPT), and total heat loss coefficient for mass flow rates of 0.01-0.07 kg/s and concentration ratios of 1–5%
- The investigation of energy efficiency, exergy efficiency, and pressure drop for minichannel FPSC operating with the nanofluids (Cu-water and TiO_2-water).

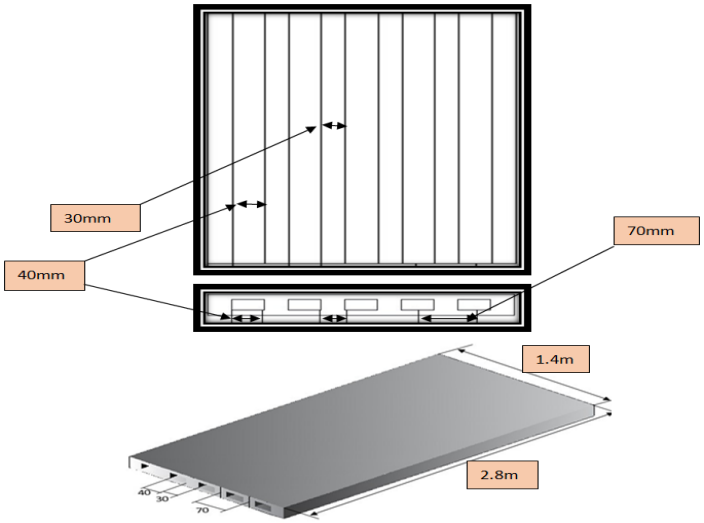

Fig.1. Schematic of MFPSC with dimensions.

Table 1 Specification of the proposed MFPSC

Parameters	Value
Thickness of absorber plate (mm)	4
Absorber plate thermal conductivity (aluminium) (W/mK)	235
Absorber plate absorptivity	0.92
Glass cover transmissivity	0.909
Absorber plate emissivity	0.09
Glass cover emissivity	0.88
Back insulation thickness (mm)	50
Side insulation Thickness (mm)	25
Insulation material thermal conductivity(W/mK)	0.025
Number of glass Cover	1
Collector tilt angle(degree)	45

Table 2 Considered metrological condition for this study

Incident solar radiation on collector G_T(W/m^2)	900
Ambient and sky temperature(^0C)	20
Speed of wind (m/s)	7

Table 3 Properties of considered nanoparticles

Properties	TiO_2	Cu
Thermal conductivity(W/mK)	8.9	400
Density(kg/m^3)	4250	8933
Heat capacity(J/kgK)	686	385

5. Methedology

This investigation comprises of four steps.1) Description of the mathematical formulations of MFPSC, 2) Description of the equations for properties of nanofluids, 3) Model validation of MFPSC 4) Parametric analysis of MFPSC with nanofluids operating for different coditions.

5.1.Mathematical formulation of MFPSC

When solar radiation of intensity G_T hit the exterior of a glass cover, some of the radiation is reflected back and some of it is absorbed by the surface of the glass, but the majority of the radiation (S) strikes the absorber plate. The absorber plate gets heated, and a part of the energy from the plate is dissipated to the surrounding area from the top surface, back surface, and side surface of the solar collector, while the remaining part of the energy (Qu) is transferred to the heat transfer fluid, which is known as useful gain. If A_c is the collector surface area, T_{pm} is the mean plate temperature (MPT), and T_a is the ambient temperature, then the useful energy gain (UEG) for FPSC in steady state can be expressed as (Deceased & Beckman, n.d.).

$$Q_u = A_c[S - U_L(T_{pm} - T_a)] \quad (1)$$

$$S = G_T(\tau\alpha)_e \quad (2)$$

$$U_L = U_t + U_b + U_e \quad (3)$$

In equation (3), U_L, U_t, U_b and U_e are known as overall heat loss coefficient (HLC), top loss coefficient, bottom loss coefficient, and edge loss coefficient, respectively and can be calculated by using following empirical formula:

$$U_t = \left(\frac{N}{\frac{C}{T_{pm}}\left(\frac{T_{pm} - T_a}{N + f}\right)^e} + \frac{1}{h_w} \right)^{-1} + \frac{\sigma\left(T_{pm} + T_a\right)\left(T_{pm}^2 + T_a^2\right)}{\frac{1}{\varepsilon_p + 0.00591Nh_w} + \frac{2N + f - 1 + 0.133\varepsilon_p}{\varepsilon_c} - N} \quad (4)$$

$$U_b = \frac{k_b}{L_b} \quad (5)$$

$$U_e = \frac{k_b}{L_e}\frac{A_e}{A_c} \quad (6)$$

Where, N, σ, T_{pm}, T_a h_w, ε_p, ε_c, L_b, L_e k_b, A_e and A_c are denoted as the number of transparent glass cover, Stefan –Boltzmann constant (5.67×10^{-8} (W/m^{2}K^4), the MPT in (K), the ambient temperature (in K), convection HTC for air (W/m^{2}K), emissivity of absorber plate, emissivity of glass cover, tilt angle of collector (degree) , thickness of back insulation (m), thickness of side insulation (m), insulation material thermal conductivity (W/mK), the side surface area and collector surface area respectively, (m^2).

If V_w is the speed of wind (m/s) then convection HTC for wind outside the cover plate can be calculated as (Deceased & Beckman, n.d.) :

$$h_w = 2.8 + 3V_w \tag{7}$$

Absorber MPT (T_{pm}) can be calculated as :

$$T_{pm} = T_i + \left(\frac{Q_u}{A_c U_L F_R}\right)\left(1 - F_R\right) \tag{8}$$

In equation (8) F is the "heat removal factor"(HRF) can be expressed as (Deceased & Beckman, n.d.) :

$$F_R = \frac{\dot{m} C_{pnf}}{A_c U_L}\left[1 - \exp\left(\frac{-A_c U_L F'}{\dot{m} C_{pnf}}\right)\right] \tag{9}$$

Where, F' is known as the "collector efficiency factor",can be represented as (Vahidinia & Khorasanizadeh, 2021):

$$F' = \left(W\left[\frac{1}{\left(a + (W-a)F\right)} + \frac{U_L}{2(a+b)h_{fi}}\right]\right)^{-1} \tag{10}$$

In equation (9) F is known as standard fin efficiency and defined as:

$$F = \frac{\tan(m(W-a)/2)}{m(W-a)/2} \tag{11}$$

Where, W, a and b are known as ,width of the unit cell, width of the minichannel and height of minichannel ,respectively.

In equation (10) m can be expressed as :

$$m = \sqrt{\frac{U_L}{k_p \delta_p}} \tag{12}$$

Convective HTC can be computed from the following relation (Vahidinia & Khorasanizadeh, 2021):

$$N_u = \frac{h_{fi} D_h}{k_f} = 4.364 + \left[0.086\left(R_e P_r\right)^{1.33} / 1 + 0.1 P_r \left(R_e P_r \frac{D_h}{L_{tube}}\right)^{0.83}\right] \tag{13}$$

Where, D_h is the minichannel's hydraulic diameter and can be represented as:

$$D_h = \frac{2ab}{a+b} \tag{14}$$

$$P_r = \frac{\mu_f C_{pf}}{k_f} \tag{15}$$

$$R_e = \frac{4\dot{m}_r}{\pi D_h \mu_f} \tag{16}$$

$$\dot{m}_r = \frac{\dot{m}}{n} \tag{17}$$

Where, n is the number of minichannel in absorber plate
The energy collection per unit length of the collector in the direction of fluid flow on both sides of the minichannel can be expressed as (Vahidinia & Khorasanizadeh, 2021) $\dot{q}_{Fin} = (W-a)F\left[S - U_L\left(T_b - T_a\right)\right]$ (18)
Total energy collection per unit cell per unit length of collector or useful energy gain in flow direction is (Vahidinia & Khorasanizadeh, 2021)

$$\dot{q}_u = WF'\left[S - U_L\left(T_{fi} - T_a\right)\right] \tag{19}$$

Water outlet temperature cab be calculated from the relation :

$$Q_u = \dot{m}C_{pf}\left(T_o - T_i\right) \tag{20}$$

The collector energy efficiency can be computed as:

$$\eta = \frac{Q_u}{A_c G_T} \tag{21}$$

5.2.Thermophysical properties of nanofluid

Thermophysical properties are based on correlation developed by various researchers on the basis of experimental studty (Geovo, Dal, Kumar, Kumar, & Roberts, 2023).

The density of the heterogeneous mixure of nanoparticle and base fluid can be calculated by following relation.

$$\rho_{nf} = \frac{\rho_{np} + \rho_{bf}(1-\varphi)}{(1-\varphi) + \frac{\varphi(d_{np} - t_{nl})^3}{d_{np}^3}} \tag{22}$$

In equation (22) d and t_{nl} are denoted for mean diameter and thickness of nano layer.
Thikness of nanolayer is:

$$t_{nl} = -0.0002833 d_{np}^2 + 0.0475 d_{np} - 0.1417 \tag{23}$$

Heat capacity of nanofluid can be expressed as

$$C_{p,nf} = \frac{1}{\rho_{nf}}\left[\rho_{nf} C_{p,np}\varphi + C_{p,bf}\rho_{bf}(1-\varphi)\right] \tag{24}$$

Viscosity of nanofluid can be calculated from following relation

$$\mu_{nf} = \mu_{bf}(1 + 7.3\varphi + 123\varphi^2) \tag{25}$$

Thermal conductivity of nanofluid can be calculated from following correlation

$$k_{nf} = [1 + \frac{5(k_{np} - k_{bf})\varphi}{k_{np} + (5-1)k_{bf} - (k_{np} - k_{bf})\varphi} \tag{26}$$

5.3.Pressure drop calculation

Calculating total head loss along a mini-channel is as follows (Vahidinia & Khorasanizadeh, 2021)]:

$$h_L = \frac{\dot{m}_r^2}{2\rho_f^2 g a^2 b^2}\left(\frac{f_{Darcy} L_{tube}}{D_h} + 1.5n\right) \quad (27)$$

Pressure drop can be calculated as (Mahian, Kianifar, Sahin, & Wongwises, 2014a)

$$\Delta P = \rho_f g(L_{tube}\sin\beta + h_L) \quad (28)$$

Pumping power for the collector can be calculated as (Vahidinia & Khorasanizadeh, 2021):

$$\text{Pumping power} = \frac{\dot{m}}{\rho_f}\Delta P \quad (29)$$

5.4.Exergy analysis

Entropy generation is the work lost by the system, which can be calculated by considering the factors leakage and destroyed exergy rate. Destroyed exergy is the summation of exergy lost due to temperature temperature difference , pressure difference and nanofluid flow in the tube. Total exegy generation of the system is(Mahian, Kianifar, Sahin, & Wongwises, 2014b):

$$\dot{S}_{gen} = \frac{\dot{W}_{lost}}{T_a} \quad (30)$$

Total work lost can be calculated as:

$$\dot{W}_{lost} = \dot{E}_d + \dot{E}_l \quad (31)$$

Destroyed exergy can be computed as :

$$\dot{E}_d = \dot{E}_{d,\Delta T_s} + \dot{E}_{d,\Delta P} + \dot{E}_{d,\Delta T_f} \quad (32)$$

$$\dot{E}_{d,\Delta T_f} = \dot{m} C_p T_a\left(\ln\left(\frac{T_{out}}{T_{in}}\right) - \frac{(T_{out} - T_{in})}{T_p}\right) \quad (33)$$

Exergy destruction brought on by temperature differences is:

$$\dot{E}_{d,\Delta T_s} = \eta_0 G_t A_c T_a\left(\frac{1}{T_p} - \frac{1}{T_s}\right) \quad (34)$$

As a result of pressure differences, the energy is destroyed when:

$$\dot{E}_{d,\Delta P} = \frac{\dot{m}\Delta P T_a \ln\left(\frac{T_{out}}{T_a}\right)}{\rho(T_{out} - T_{in})} \quad (35)$$

The exergy that is lost as a result of fluid flow in the collector is:

$$\dot{E}_{d,\Delta T_f} = \dot{m} C_p T_a\left(\ln\left(\frac{T_{out}}{T_{in}}\right) - \frac{(T_{out} - T_{in})}{T_p}\right) \quad (36)$$

Leakage exergy can be calculated as:

$$\dot{E}_l = U_L A_c (T_p - T_a)\left(1 - \frac{T_a}{T_p}\right) \quad (37)$$

Total entropy generation (as in Eq.38) of the system can be calculated after substituting the equation (31)-(37) in equation (30)

$$\dot{S}_{gen} = \eta_o G_t A_c \left(\frac{1}{T_p} - \frac{1}{T_s} \right) + \dot{m} C_p \left(\ln(\frac{T_{out}}{T_{in}}) - \frac{(T_{out} - T_{in})}{T_p} \right) + U_L A_c (1 - \frac{T_a}{T_p})(\frac{T_p}{T_a} - 1)$$

$$+ \frac{\dot{m} \Delta P}{\rho_{nf} (T_{out} - T_{in})} \ln(\frac{T_{out}}{T_a}) \quad (38)$$

The exergy destruction of the system can be calculated by using eq.(39)

$$\dot{E}_{dest} = T_a \dot{S}_{gen} \quad (39)$$

The exergy efficiency of the system can be expressed by eq. (40) (Said, Sabiha, Saidur, Hepbasli, Rahim, & Mekhilef, 2015).

$$\eta_{exer} = 1 - \frac{\dot{E}_{dest}}{\left[1 - (\frac{T_a}{T_{sol}}) \right] \dot{Q}_{sol}} \quad (40)$$

In equation (40) T_{sol} is the defined as the apparent surface temperature of the surface of the sun and $Q_{sol} = G_T(\tau\alpha)A_c$ The above equations are non-linear algebraic equations that cannot be solved by the analytical method. In order to solve these equations, an iterative approach using energy equation solver software has been used. Initially, the MPT is assumed, and equations are solved to calculate different parameters. By updating guess values and applying energy balance for MFPSC, a convergent value of the MPT is obtained. At the converged temperature, different parameters like fluid outlet temperature, HRF, useful energy gain, and thermal efficiency have been computed.

6. Result and discussion

In this section, the performance of MFPSC for two nanofluids (TiO_2-water and Cu-water) with different concentrations has been evaluated and compared considering different parameters like water outlet temperature, absorber MPT, overall HLC, HRF, energy efficiency, and exergy efficiency for different MFRs, concentrations, and water inlet temperatures. Fig. 2 shows the variation of the MPT of the current study and that of Vahidinia & Khorasanizadeh (2021) according to MFR. As seen in the figure, there is a good agreement between the two sets of data. It can be observed in Table 4 that the predicted output values of different parameters of the present study and those of the literature for MFR of 0.033 kg/s and water inlet temperature of 320K. The percentage relative changes for water outlet temperature, MPT, HRF, overall HLC, and useful heat gain are 2.54, 4.32, 1.66, 0.392, 0.075, and 0.058, respectively. The percentage relative change does not exceed more than 4.32 for any parameter, which indicates excellent agreement between the present study and that of Vahidinia & Khorasanizadeh(2021).Table.5 depicts the various output parameters for both the nanofluids at MFR of 0.01kg/s and 0.07kg/s and concentration ratio of 1% and 5% by volume at an inlet temperature of 320K.

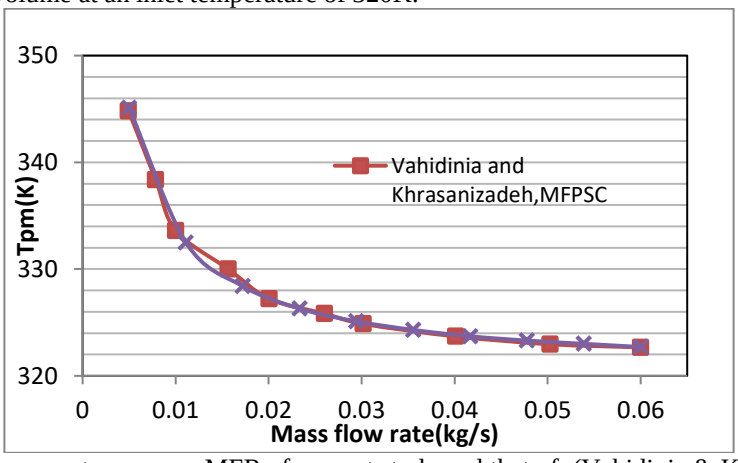

Fig.2.The mean plate temperature versus MFR of present study and that of (Vahidinia & Khorasanizadeh, 2021).

Table 4. Comparison of different parameters of the present study with (Vahidinia & Khorasanizadeh, 2021)

Parameter	Present Study	(Vahidinia & Khorasanizadeh, 2021)	Relative change%
$T_o(^0C)$	55.7	54.3	2.545455
$T_{pm}(^0C)$	49.6	47.5	4.325438
F_R	0.971	0.955	1.661475
$U_L(W/m^2K)$	3.825	3.81	0.392927
	0.6645	0.664	0.075273
$Q_u(W)$	1196	1195.3	0.058546

Table 5. Comparison of different output parameters for the nanofluids at different MFR and concentration ratio

TiO_2-water												
ϕ=1%							ϕ =5%					
m (kg/s)	T_o(K)	T_{pm}(K)	U_L(W/m^{2}K)	HRF	η	η_{ex}	T_o(K)	T_{pm}(K)	U_L(W/m^{2}K)	HRF	η	η_{ex}
0.01	369.4	347.9	4.294	0.8142	0.5828	0.2029	395.9	351.1	4.335	0.7902	0.5646	0.2227
0.07	330.3	325.2	3.938	0.9688	0.7039	0.1865	331.8	325.7	3.948	0.9654	0.701	0.1881
Cu-water												
ϕ =1%							ϕ =5%					
m (kg/s)	T_o(K)	T_{pm}(K)	U_L(W/m^{2}K)	HRF	η	η_{ex}	T_o(K)	T_{pm}(K)	U_L(W/m^{2}K)	HRF	η	η_{ex}
0.01	400.6	348.9	4.307	0.8067	0.5772	0.2357	417	355.9	4.394	0.7582	0.5378	0.2352
0.07	330.7	325.4	3.941	0.9677	0.7029	0.187	334.1	326.7	3.966	0.9596	0.6964	0.1902

6.1. Effect of MFR on the performance of MFPSC

For two different nanofluids, TiO_2-water and Cu-water, Fig. 3 illustrates the variation of fluid outlet temperature with regard to MFR. At concentration ratios of 1% and 5%, both nanofluids are utilised. It is found that the temperature of the fluid outlets for both fluids drops as the MFR rises. Heat transfer fluid has a lower temperature at a higher MFR because it absorbs less heat there. Additionally, for both the concentration ratios of 1% and 5%, it can be seen that the fluid outlet temperature of the Cu-water nanofluid is higher than that of the TiO_2-water nanofluid. It can be explained by the fact that the heat capacity has an important effect on the fluid output temperature. The fluid outlet temperature will be low if the heat capacity is high. Compared to TiO_2-water nanofluid, Cu-water nanofluid has a lower heat capacity. As a result, the outlet temperature for the nanofluid Cu-water is higher than for the nanofluid TiO_2-water.

Fig. 4 illustrates the variation of the MPT of the absorber plate according to the MFR of nanofluids. As seen, the MPT decreases as the MFR increases for both nanofluids. At a higher MFR , turbulence is high, and due to high turbulence, convection heat transfer coefficient between plate surface and fluid is enhanced, increasing heat transfer rate. A high heat transfer rate to the fluid decreases the MPT, and the overall HLC decreases accordingly, as shown in Fig. 5. As seen in Figs. 4 and 5, for all MFRs, the MPT and overall HLC for the fluid 5% Cu-water have the highest values, and that is lowest for 1% TiO_2-water. It can be explained as follows: due to the low heat capacity of 5% Cu-water nanofluid, less heat is absorbed by the fluid, which increases the MPT as well as the overall heat transfer coefficient.

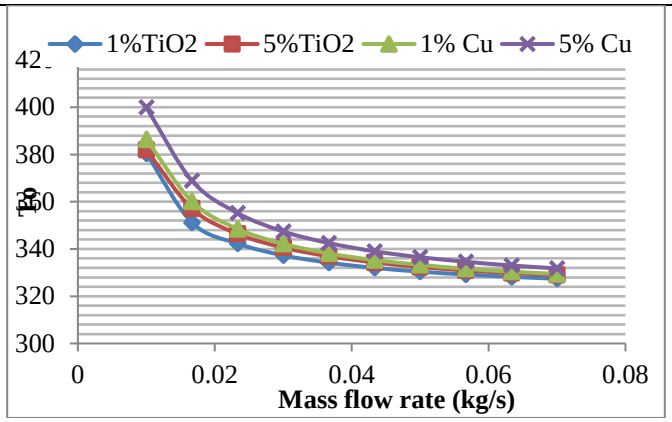

Fig.3.Variations of water outlet temperature v/s MFR

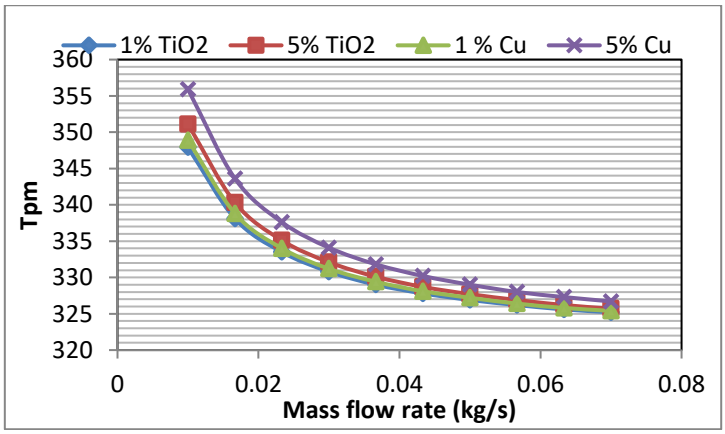

Fig.4.variation of mean plate temperature v/s MFR

Figs. 6 and 7 demonstrate the effect of MFR for both nanofluids on the HRF and energy efficiency of MFPSC. As seen in the figure, as the MFR increases, the HRF and energy efficiency of the collector increase for all fluids. At lower MFRs, the variation of HRF and energy efficiency is high, but at higher MFRs, changes for both factors are almost asymptotically large. Since flow velocity and Reynolds number increase with increasing MFR, convective heat transfer is increased, and heat transfer rate is enhanced. A higher heat transfer rate reduces the MPT and consequently decreases the overall HLC. Due to the fact that HRF and energy efficiency increase with increasing MFRs. It can also be noted that efficiency and HRF are invariant for concentration ratio at higher MFRs, but at lower MFRs, the efficiency and HRF for 1% TiO_2-water nanofluid are greater than those for the other mentioned fluids

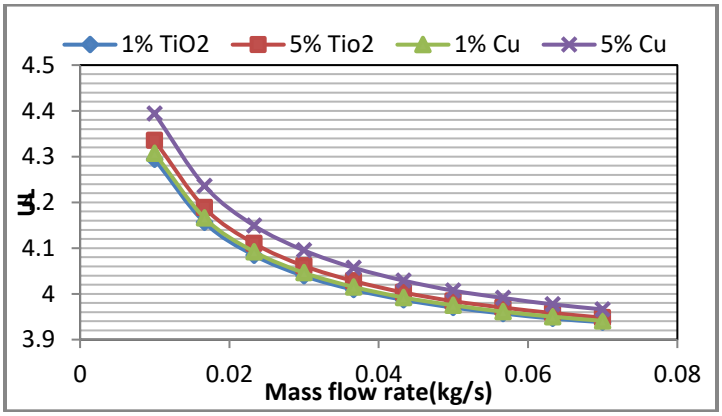

Fig.5.variation of overall heat loss cofficient v/s MFR

Fig. 8 illustrates the variation of exergy efficiency according to MFR for the selected fluids at concentrations of 1% and 5%. Exergy efficiency for 5% Cu-water nanofluid is higher than that of other considered fluids for MFRs of 0.01 to 0.08 kg/s. Since energy efficiency depends on the heat capacity of the fluid and the overall HLC, The heat capacity of a 5% Cu-water nanofluid is lower than the other considered nanofluids, and the overall HLC of 5% Cu-water is higher than the other considered fluids. Due to the lower heat capacity, the energy destroyed by the nanofluid is also lower.

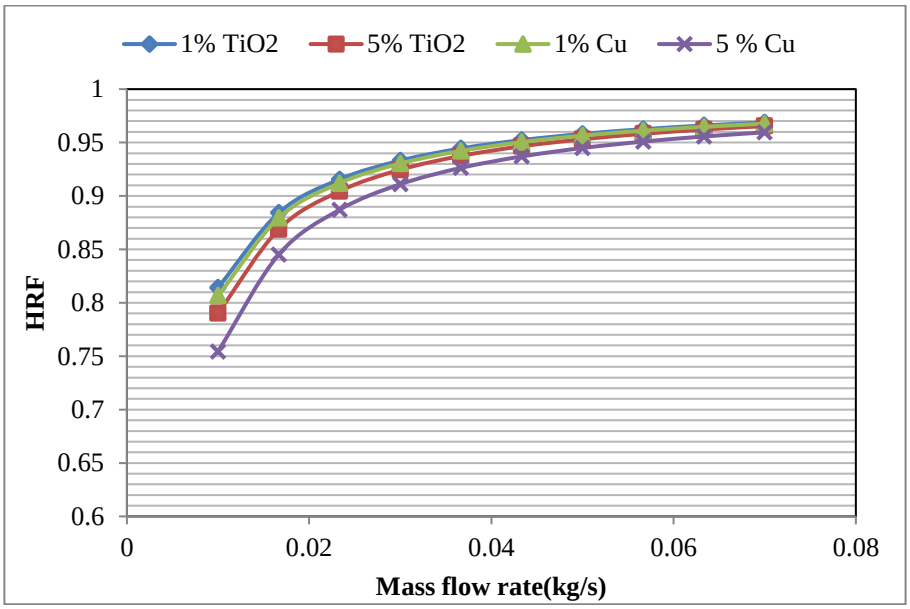

Fig.6.variation of heat removal factor v/s MFR

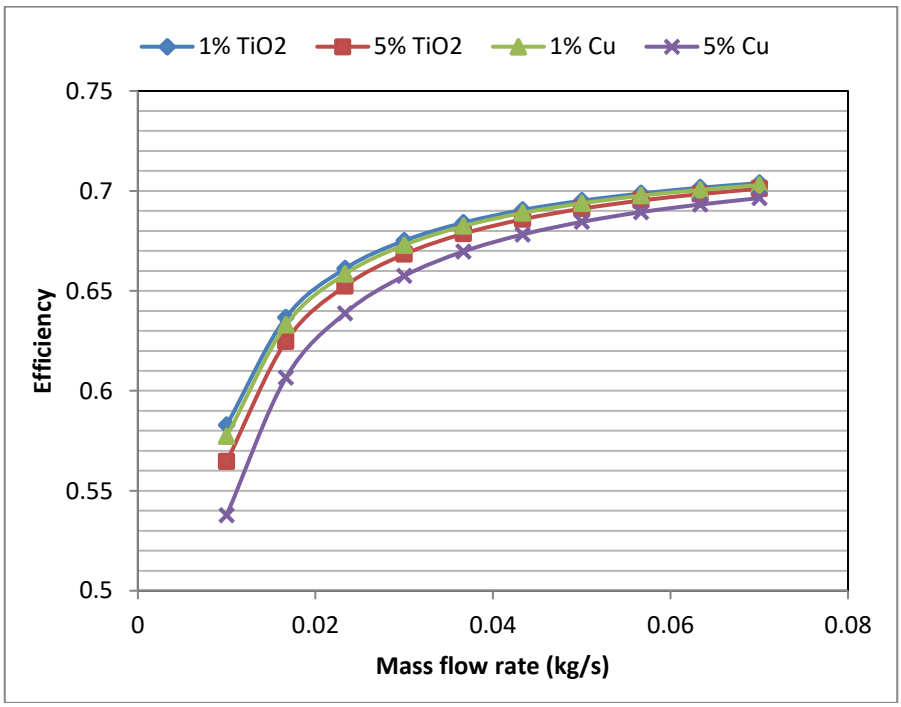

Fig.7.variation of energy efficiency v/s MFR

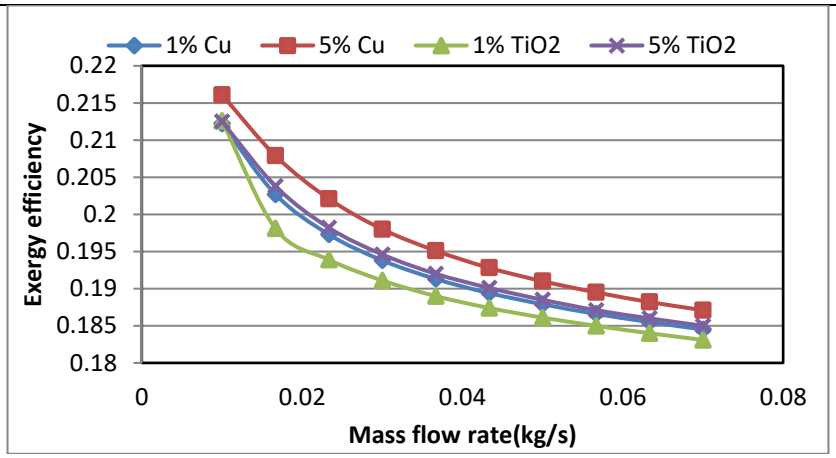

Fig.8.variation of exergy efficiency v/s MFR

6.2. Effect of volumetric ratio on the performance of MFPSC

Fig. 9 demonstrates the variation of fluid outlet temperature according to volumetric ratio for considered nanofluids with two different MFRs. It is clear that the outlet temperature increases with increasing volumetric ratio, and the outlet temperature for Cu-water nanofluid is higher as compared to TiO_2-water nanofluid for MFRs of 0.01 kg/s and 0.07 kg/s, respectively. The outlet temperature strongly depends on heat capacity; the lower the heat capacity, the higher the outlet temperature. Hence, the outlet temperature for Cu-water nanofluid is higher as compared to TiO_2-water nanofluid for MFRs of 0.01 and 0.07 kg/s. As observed, with a flow rate of 0.01 kg/s, the variation of outlet temperature is greater as compared to 0.07 kg/s with increasing the volumetric ratio. Because at a lower MFR, the absorption of heat energy is greater. It is known that the higher the density, the lower the velocity of the fluid at a constant MFR, and the fluid will absorb more thermal energy. Since the density of the Cu-water nanofluid is higher than the TiO_2-water nanofluid.

Figs. 10 and 11 show the variation of MPT and overall HLC with respect to the volumetric ratio of both the nanofluids at MFRs of 0.01 and 0.07 kg/s. As the volumetric ratio increases, the overall HLC and MPT of both nanofluids increase. When volumetric ratio increases, the viscosity of nanofluid increases, and the greater the viscous force, the lower the heat transfer coefficient between nanofluid and plate surface. Lower heat transfer coefficients increase the overall HLC and MPT. As noticed, the MPT and overall HLC for Cu-water nanofluid are higher as compared to TiO_2-water nanofluid for MFRs of 0.01 and 0.07 kg/s, It may be due to the fact that the Prandtl number of Cu-water nanofluid is lower than that of TiO_2-water nanofluid. At a MFR of 0.07 kg/s, the difference between the MPT and the overall HLC for both fluids is very low because of the high heat transfer coefficient. At higher MFRs, heat transfer coefficients increase due to turbulence, which is predominant over the viscous effect.

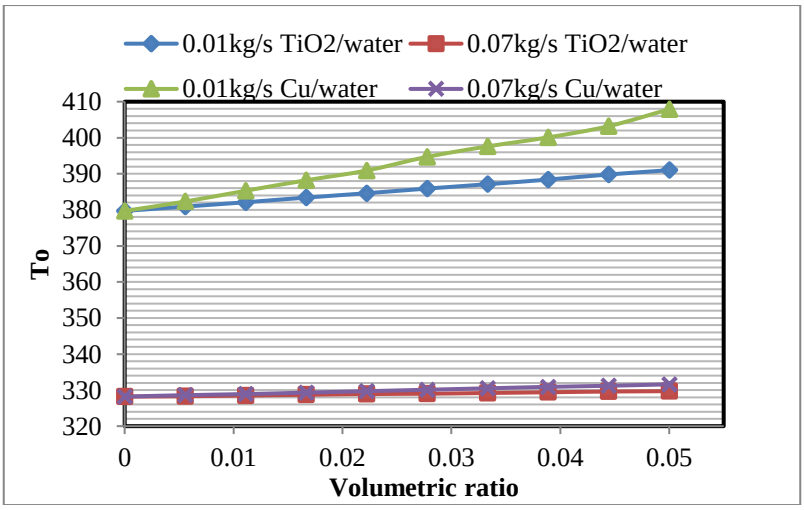

Fig.9.Variation of fluid outlet temperature v/s volumetric ratio

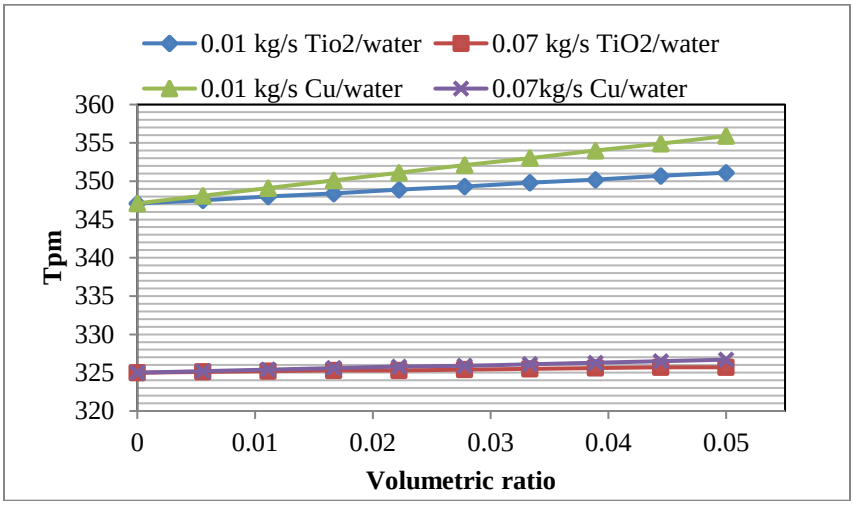

Fig.10.Variation of mean plate temperature v/s volumetric ratio

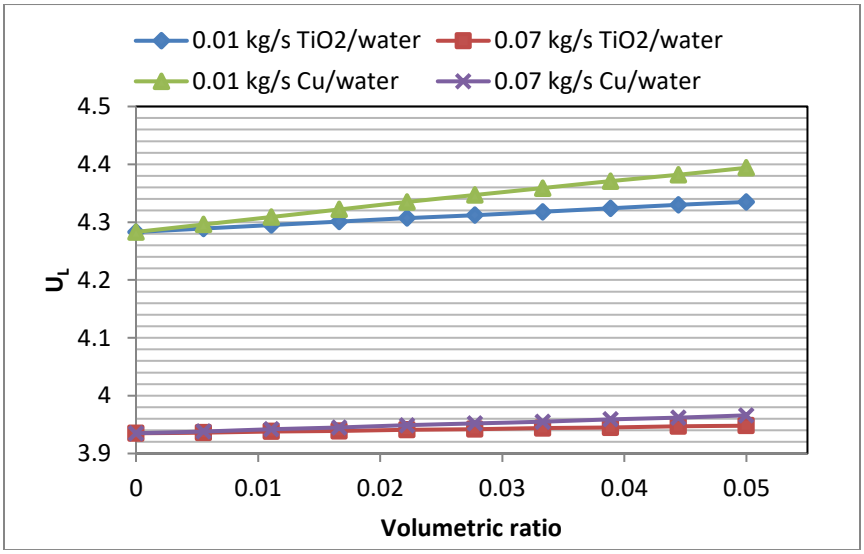

Fig.11.Variation of overall heat loss coefficient v/s volumetric ratio

Fig.12. Demonstrate the variation of energy efficiency according to volumetric ratio of considered nafluids for MFRs of 0.01 kg/s and 0.07 kg/s. It can be observed that the efficiency of nanofluid at a MFR of 0.07 kg/s is greater than that of 0.01 kg/s. Because at higher MFRs the heat transfer rate is enhanced due to high turbulence, efficiency at higher MFRs is high. Efficiency decreases with increasing volumetric ratio for both considered nanofluids because of the decreasing trend of MPT and overall HLC, as shown in figs. 10 and 11. The efficiency of TiO_2-water nanofluid is greater than that of Cu-water nanofluid at both MFRs because of lower MPT and overall heat transfer.

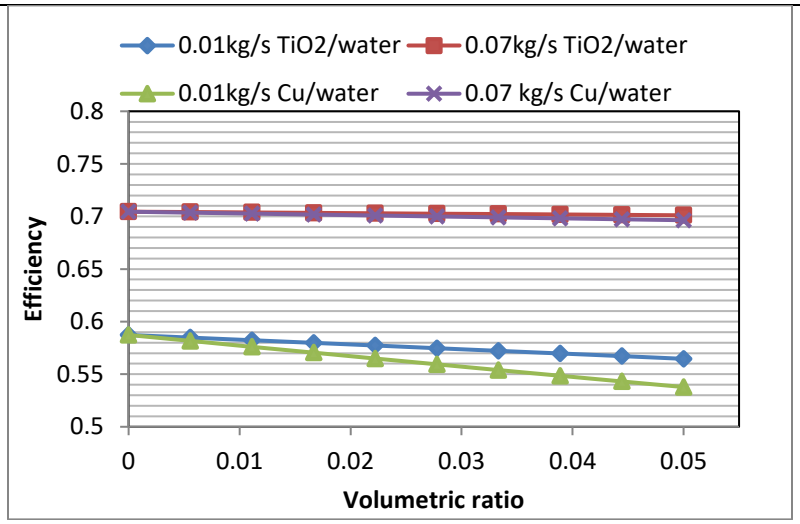

Fig.12.Variation of energy efficiency v/s volumetric ratio

The variation of exergy efficiency with respect to the volumetric ratio of considered nanofluids for two different MFRs is presented in Fig. 13. As seen in the figure, exergy efficiency increases with increasing volumetric ratios of considered nanofluids at MFRs of 0.01 and 0.07 kg/s. It can be explained as MPT increasing with increasing volumetric ratio, and according to Eq. (38) entropy generation will decrease when MPT increases. The smaller the entropy generation, the lower will be the exergy destroyed, and consequently, the larger will be the exergy efficiency. That is why the exergy efficiency increases as the volumetric ratio increases for both MFR. A graph of exergy destroyed versus volumetric ratio can be seen in Fig. 14. It can also be noted that the exergy efficiency at a MFR of 0.07kg/s is lower than that of 0.01 kg/s. Since at a higher MFR the MPT is lower and the pressure drop is higher, according to Eq. 38, entropy generation is high. Therefore, exergy efficiency at a higher MFR is lower. The MPT for the Cu-water nanofluid is greater than that of the TiO_2-water nanofluid, which is why the exergy efficiency for the Cu-water nanofluid is greater than that of the TiO_2-water nanofluid for MFRs of 0.01kg/s and 0.07kg/s.

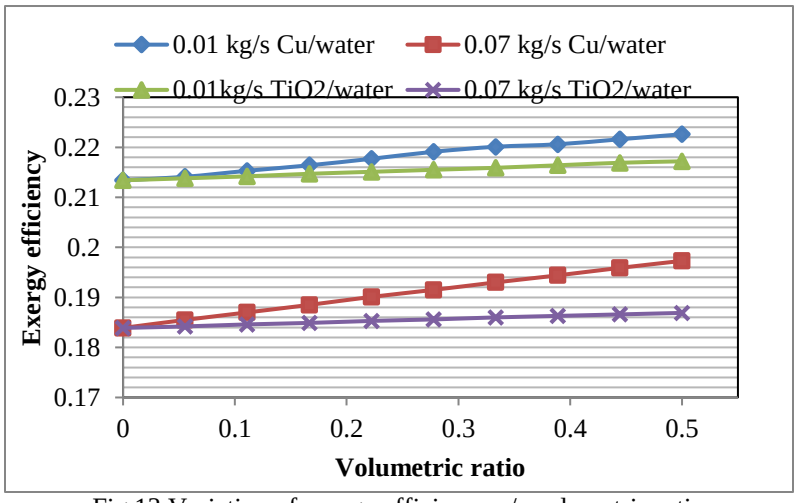

Fig.13.Variation of exergy efficiency v/s volumetric ratio

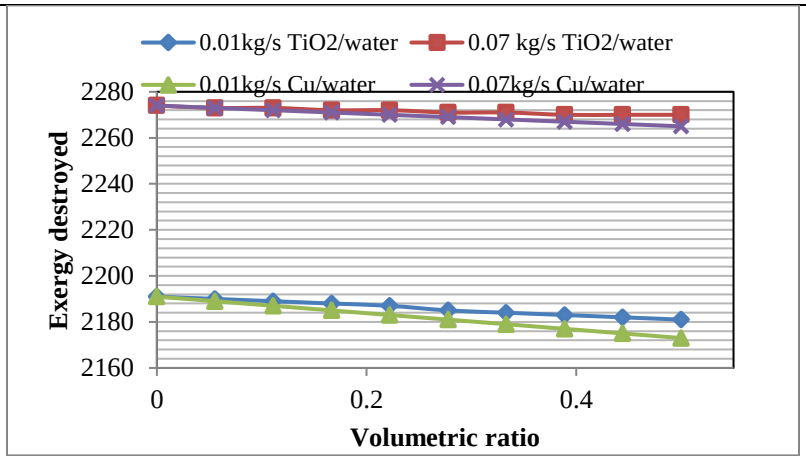

Fig.14.Variation of exergy destroyed v/s volumetric ratio

6.3.Hydraulic performance of a minichannel flat plate solar collector

Figs. 15 and 16 show the variation of pressure drop for different volumetric ratios of nanofluid TiO_2-water and Cu-water. As seen in the figure, it is clear that pressure drop increases with increasing volumetric ratios for both nanofluids. Because the viscosity of the nanofluid increases due to nanoparticle loading, the pressure drop increases with increasing volumetric ration. It can also be noted that the pressure drop for the nanofluid Cu-water is greater than that of the TiO_2-water nanofluid. From Eq. (28), it is clear that the pressure drop depends on total head loss and the density of the nanofluid. For large minichannels, the pressure drop due to head loss is significantly lower than that of the density factor. Since the density of Cu-water nanofluid is greater than that of TiO_2-water for the considered volumetric ratio, Due to the fact that the pressure drop for the nanofluid Cu-water is greater than the TiO_2-water.

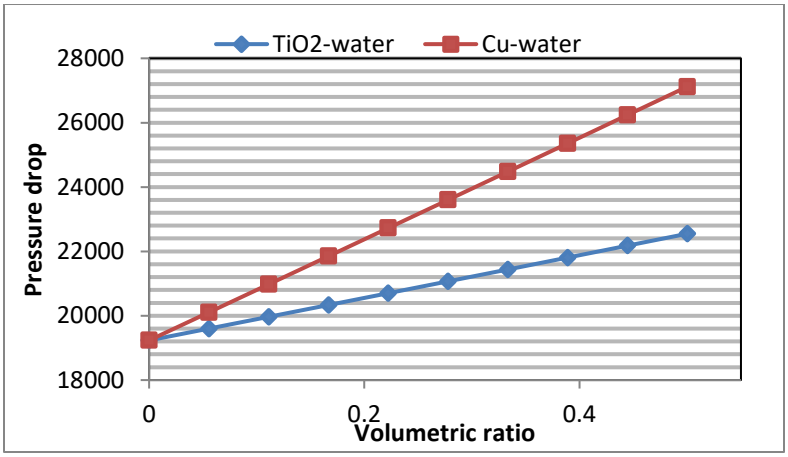

Fig.15.Variation of pressure drop v/s volumetric ratio for MFR of 0.01kg/s

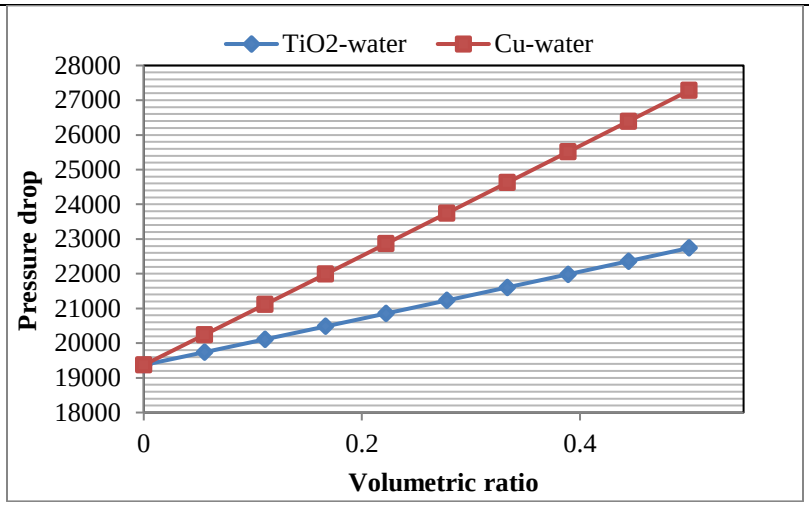

Fig.16.Variation of pressure drop v/s volumetric ratio for MFR of 0.07kg/s

6.4. Effect of inlet temperature on the performance of MFPSCS

Fig. 17 shows the variation of energy efficiency of MFPSC according to reduced temperature for different concentrations of nanofluid at a MFR of 0.7 kg/s. As seen in the figure, for a constant ambient temperature, energy efficiency decreases as the inlet temperature of nanofluids increases. At higher inlet temperatures, the overall HLC will be high, and consequently, the energy efficiency will be lower. It can also be noticed that the energy efficiency of the collector for 1% TiO_2-water nanofluid is highest and for 5% Cu-water nanofluid is lowest. For a constant MFR, the MPT for the nanofluid 1% TiO_2-water is lowest and for the nanofluid 5% Cu-water is highest, so heat loss for the 5% Cu-warer nanofluid will be highest. That is why the energy efficiency of Cu-water nanofluid is lower than that of TiO_2-water for the same MFR.

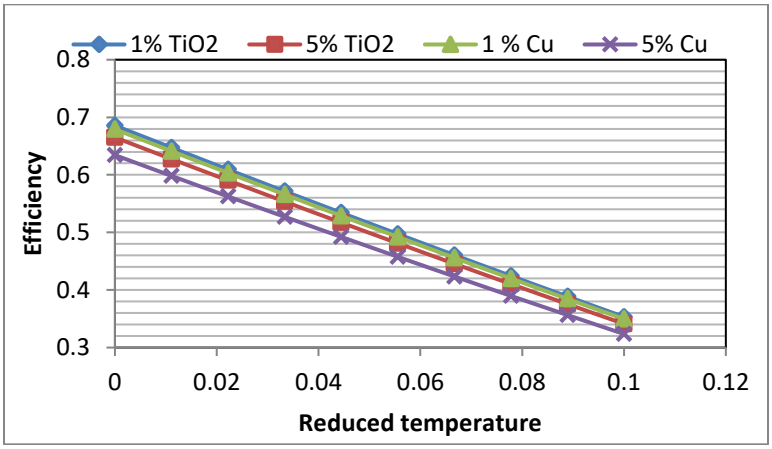

Fig.17.Variation of Efficiency v/s reduced temperature for MFR of 0.07kg/s

7. Conclusion

Thermo physical properties of a MFPSC of dimension (2800 mm X 1400 X 4mm) with rectangular channel of width 40mm,depth 2mm and spacing between two consecutive channel is 30mm have been analyzed using two different nanofluids Cu-water and TiO_2-water. The results of this study are presented for MFR from 0.01 to 0.07kg/s and volumetric ratio of the nanofluid from 1% to 5% at inlet temperature of 320K. The findings of this study are summarized as follows:

- The outlet temperature of a nanofluid depends on its MFR, density, concentration, and heat capacity. But outlet temperature strongly depends on the heat capacity of the nanofluid.

- The heat capacity of Cu-water nanofluid is lower than that of TiO_2-water. Therefore, the outlet temperature for Cu-water nanofluid is 31.2 degrees greater than the TiO_2-water nanofluid for a 1% volumetric ratio and a 0.01 kg/sMFR.
- The outlet temperature and MPT increase with increasing volumetric ratio for considered nanofluids at a constant MFR. The outlet temperature and MPT for the nanofluid TiO_2-water of volumetric ratio 1% are 369.4K and 347.9 K, respectively, and these values increase to 395.9K and 351.1K at volumetric ratio of 5% for the same MFR of 0.01 kg/s.
- The MPT is always less than the outlet temperature of the nanofluid due to direct contact of the fluid with the plate.
- The overall HLC of MFPSC for Cu-water nanofluid is greater than that of TiO_2-water nanofluid for the same MFR and concentration ratio.
- The HRF and energy efficiency of MFPSC depend on the MFR, volumetric ratio, and nature of fluids. The HRF and efficiency of the collector for TiO_2-water nanofluid are greater than those for Cu-water for the same concentration ratio and MFR. For both the nanofluids, the HRF and energy decrease as the volumetric ratio increases from 1% to 5%.
- At a higher MFR of 0.07 kg/s, the HRF and energy efficiency of MFPSC for both nanofluids are greater than those at a lower MFR of 0.01 kg/s.
- By increasing the concentration of nanoparticles, the exergy efficiency is enhanced for the same MFR for both nanofluids. The exergy efficiency of Cu-water nanofluid is greater than that of TiO_2-water nanofluid for the same concentration ratio andMFR.
- Loading the nanoparts into the base fluid increases the viscosity of the nanofluid, and consequently, the pressure drop. It is also found that the pressure drop for the Cu-water nanofluid is greater than that of TiO_2-water for the same MFR in the range of volumetric ratios from 0 to 5%.

Today, the application of nanofluid in the field of solar technology increases day by day due to its capability to enhance the thermophysical properties of heat transfer fluid. The thermophysical properties of fluids affect the performance of the solar collector. There are some possibilities for work that needs to be done, as follows:

- Comparative analysis can be done for different shapes of MFPSCs.
- Some more studies are required for the performance measurement of MFPSC by using different mono and hybrid nanofluids.
- Correlations for some parameters like the Nusselts number and friction factor need to be developed.

Declaration of competing interest: The authors acknowledge that they have no known financial or interpersonal conflicts that would have appeared to have an impact on the research contained in this study.

8. References

[1] Abu-hamdeh, N. H., Alazwari, M. A., Salilih, E. M., Sajadi, S. M., & Karimipour, A. (2021). Improve the efficiency and heat transfer rate ' trend prediction of a flat-plate solar collector via a solar energy installation by examine the Titanium Dioxide / Silicon Dioxide-water nanofluid. *Sustainable Energy Technologies and Assessments*, *48*(June), 101623. https://doi.org/10.1016/j.seta.2021.101623

[2] Akram, N., Montazer, E., Kazi, S. N., Elahi, M., Soudagar, M., Ahmed, W., … García, M. (2021). *Experimental investigations of the performance of a fl at-plate solar collector using carbon and metal oxides based nano fl uids*. *227*. https://doi.org/10.1016/j.energy.2021.120452

[3] Alawi, O. A., Mohamed, H., Mallah, A. R., Mohammed, H. A., Kazi, S. N., Azwadi, N., … Naja, G. (2021). *Nano fl uids for fl at plate solar collectors : Fundamentals and applications*. *291*. https://doi.org/10.1016/j.jclepro.2020.125725

[4] Allouhi, A., & Amine, M. B. (2021). Solar Energy Materials and Solar Cells Heat pipe flat plate solar collectors operating with nanofluids. *Solar Energy Materials and Solar Cells*, *219*(March 2020), 110798. https://doi.org/10.1016/j.solmat.2020.110798

[5] Arvanitis, K. D., Papanicolaou, E., Mathioulakis, E., Belessiotis, V., & Bouris, D. (2020). Experimental evaluation of flat-plate heat absorbers for medium-temperature linear-focus solar systems: composite U-bends vs straight rectangular-multi-channels. *Applied Thermal Engineering*, 115364.

https://doi.org/10.1016/j.applthermaleng.2020.115364

[6] Bagher, M., Saedodin, S., Hadi, S., Doostmohammadi, M., & Khaledi, O. (2022). The effect of vortex generator insert and TiO 2 / Water nanofluid on thermal efficiency and heat transfer of flat plate solar collector. *Sustainable Energy Technologies and Assessments*, *53*(PC), 102617. https://doi.org/10.1016/j.seta.2022.102617

[7] Bezaatpour, M., & Rostamzadeh, H. (2021). Design and evaluation of fl at plate solar collector equipped with nano fl uid , rotary tube , and magnetic fi eld inducer in a cold region. *Renewable Energy*, *170*, 574–586. https://doi.org/10.1016/j.renene.2021.02.001

[8] Deceased, J. A. D., & Beckman, W. A. (n.d.). *of Thermal Processes Solar Engineering*.

[9] Dobriyal, R., Negi, P., Sengar, N., & Singh, D. B. (2019). Materials Today : Proceedings A brief review on solar flat plate collector by incorporating the effect of nanofluid. *Materials Today: Proceedings*, (xxxx). https://doi.org/10.1016/j.matpr.2019.11.294

[10] Farhana, K., Kadirgama, K., Mohammed, H. A., Ramasamy, D., Samykano, M., & Saidur, R. (2021). Analysis of efficiency enhancement of flat plate solar collector using crystal nano-cellulose (CNC) nanofluids. *Sustainable Energy Technologies and Assessments*, *45*(February), 101049. https://doi.org/10.1016/j.seta.2021.101049

[11] Geovo, L., Dal, G., Kumar, R., Kumar, S., & Roberts, J. J. (2023). *Theoretical model for flat plate solar collectors operating with nanofluids : Case study for Porto Alegre , Brazil*. *263*(October 2022). https://doi.org/10.1016/j.energy.2022.125698

[12] He, Q., Zeng, S., & Wang, S. (2015). *Experimental investigation on the ef fi ciency of fl at-plate solar collectors with nano fl uids*. *88*, 165–171. https://doi.org/10.1016/j.applthermaleng.2014.09.053

[13] Jabari, A., Farzane-gord, M., Sajadi, M., & Hoseyn-zadeh, M. (2014). Effects of CuO / water nanofluid on the efficiency of a flat-plate solar collector. *EXPERIMENTAL THERMAL AND FLUID SCIENCE*, *58*, 9–14. https://doi.org/10.1016/j.expthermflusci.2014.06.014

[14] Javadi, F. S., Saidur, R., & Kamalisarvestani, M. (2013). Investigating performance improvement of solar collectors by using nano fl uids. *Renewable and Sustainable Energy Reviews*, *28*, 232–245. https://doi.org/10.1016/j.rser.2013.06.053

[15] Khin, N., Sint, C., Choudhury, I. A., Masjuki, H. H., & Aoyama, H. (2017). Theoretical analysis to determine the efficiency of a CuO-water nanofluid based-flat plate solar collector for domestic solar water heating system in Myanmar. *Solar Energy*, *155*, 608–619. https://doi.org/10.1016/j.solener.2017.06.055

[16] Mahian, O., Kianifar, A., Sahin, A. Z., & Wongwises, S. (2014a). International Journal of Heat and Mass Transfer Entropy generation during Al 2 O 3 / water nanofluid flow in a solar collector : Effects of tube roughness , nanoparticle size , and different thermophysical models. *HEAT AND MASS TRANSFER*, *78*, 64–75. https://doi.org/10.1016/j.ijheatmasstransfer.2014.06.051

[17] Mahian, O., Kianifar, A., Sahin, A. Z., & Wongwises, S. (2014b). Performance analysis of a minichannel-based solar collector using different nanofluids. *Energy Conversion and Management*, *88*, 129–138. https://doi.org/10.1016/j.enconman.2014.08.021

[18] Mansour, M. K. (2013). Thermal analysis of novel minichannel-based solar fl at-plate collector. *Energy*, *60*, 333–343. https://doi.org/10.1016/j.energy.2013.08.013

[19] Mete, A., Akif, M., & Turgut, A. (2018). Thermal performance of a nanofluid-based flat plate solar collector : A transient numerical study. *Applied Thermal Engineering*, *130*, 395–407. https://doi.org/10.1016/j.applthermaleng.2017.10.166

[20] Mohan, S., Dinesha, P., & Iyengar, A. S. (2021). Modeling and analysis of a solar minichannel flat plate collector system and optimization of operating conditions using particle swarms. *Thermal Science and Engineering Progress*, *22*(September 2020), 100855. https://doi.org/10.1016/j.tsep.2021.100855

[21] Moravej, M., Vahabzadeh, M., Guan, Y., & Li, L. K. B. (2020). *Enhancing the e ffi ciency of a symmetric fl at-plate solar collector via the use of rutile TiO 2 -water nano fl uids*. *40*(May). https://doi.org/10.1016/j.seta.2020.100783

[22] Muhammad, M. J., Muhammad, I. A., Azwadi, N., Sidik, C., Noor, M., & Muhammad, W. (2016). *Thermal performance enhancement of fl at-plate and evacuated tube solar collectors using nano fl uid : A review ☆*. *76*, 6–15. https://doi.org/10.1016/j.icheatmasstransfer.2016.05.009

[23] Murugan, M., Saravanan, A., Elumalai, P. V, Kumar, P., Saleel, C. A., David, O., … Afzal, A. (2022). An overview on energy and exergy analysis of solar thermal collectors with passive performance enhancers. *Alexandria Engineering Journal*, *61*(10), 8123–8147. https://doi.org/10.1016/j.aej.2022.01.052

[24] Mustafa, J., Alqaed, S., & Sharifpur, M. (2022). Evaluation of energy efficiency , visualized energy , and production of environmental pollutants of a solar flat plate collector containing hybrid nanofluid. *Sustainable Energy Technologies and Assessments*, *53*(PA), 102399. https://doi.org/10.1016/j.seta.2022.102399

[25] Nabi, H., Pourfallah, M., Gholinia, M., & Jahanian, O. (2022). Case Studies in Thermal Engineering Increasing heat transfer in flat plate solar collectors using various forms of turbulence-inducing elements and CNTs-CuO hybrid nanofluids. *Case Studies in Thermal Engineering*, *33*(March), 101909. https://doi.org/10.1016/j.csite.2022.101909

[26] Oyinlola, M. A., Shire, G. S. F., & Moss, R. W. (2015). International Journal of Heat and Mass Transfer Investigating the effects of geometry in solar thermal absorber plates with micro-channels. *HEAT AND MASS TRANSFER*, *90*, 552–560. https://doi.org/10.1016/j.ijheatmasstransfer.2015.06.087

[27] Raj, P., & Subudhi, S. (2018). A review of studies using nano fl uids in fl at-plate and direct absorption solar collectors. *Renewable and Sustainable Energy Reviews*, *84*(September 2016), 54–74. https://doi.org/10.1016/j.rser.2017.10.012

[28] Robles, A., Duong, V., Martin, A. J., Guadarrama, J. L., & Diaz, G. (2014). ScienceDirect Aluminum minichannel solar water heater performance under year-round weather conditions. *SOLAR ENERGY*, *110*, 356–364. https://doi.org/10.1016/j.solener.2014.09.031

[29] Sadeghinezhad, E., Mehrali, M., Saidur, R., Mehrali, M., Tahan, S., Reza, A., … Metselaar, C. (2016). A comprehensive review on graphene nanofluids : Recent research , development and applications. *ENERGY CONVERSION AND MANAGEMENT*, *111*, 466–487. https://doi.org/10.1016/j.enconman.2016.01.004

[30] Said, Z., Sabiha, M. A., Saidur, R., Hepbasli, A., Rahim, N. A., & Mekhilef, S. (2015). Performance enhancement of a Flat Plate Solar collector using Titanium dioxide nano fl uid and Polyethylene Glycol dispersant. *Journal of Cleaner Production*, *92*, 343–353. https://doi.org/10.1016/j.jclepro.2015.01.007

[31] Said, Z., Sabiha, M. A., Saidur, R., Hepbasli, A., Rahim, N. A., Mekhilef, S., & Ward, T. A. (2015). Performance enhancement of a Flat Plate Solar collector using TiO_2 nanofluid and Polyethylene Glycol dispersant. *Journal of Cleaner Production*. https://doi.org/10.1016/j.jclepro.2015.01.007

[32] Said, Z., Saidur, R., & Rahim, N. A. (2016). Energy and exergy analysis of a flat plate solar collector using different sizes of Aluminium oxide based nanofluid. *Journal of Cleaner Production*. https://doi.org/10.1016/j.jclepro.2016.05.178

[33] Sami, W., Kazi, S. N., & Badarudin, A. (2015). ScienceDirect A review of studies on using nanofluids in flat-plate solar collectors. *Solar Energy*, *122*, 1245–1265. https://doi.org/10.1016/j.solener.2015.10.032

[34] Sharafeldin, M. A., & Gróf, G. (2018). Experimental investigation of fl at plate solar collector using CeO 2 - water nano fl uid. *Energy Conversion and Management*, *155*(October 2017), 32–41. https://doi.org/10.1016/j.enconman.2017.10.070

[35] Sharma, N., & Diaz, G. (2011). Performance model of a novel evacuated-tube solar collector based on minichannels. *Solar Energy*, *85*(5), 881–890. https://doi.org/10.1016/j.solener.2011.02.001

[36] Sheikholeslami, M., Ali, S., Ebrahimpour, Z., & Said, Z. (2021). Recent progress on fl at plate solar collectors and photovoltaic systems in the presence of nano fl uid : A review. *Journal of Cleaner Production*, *293*, 126119. https://doi.org/10.1016/j.jclepro.2021.126119

[37] Sundar, L. S., Kirubeil, A., Punnaiah, V., Singh, M. K., & Sousa, A. C. M. (2018). International Journal of Heat and Mass Transfer Effectiveness analysis of solar flat plate collector with Al 2 O 3 water nanofluids and with longitudinal strip inserts. *International Journal of Heat and Mass Transfer*, *127*, 422–435. https://doi.org/10.1016/j.ijheatmasstransfer.2018.08.025

[38] Sundar, L. S., Misganaw, A. H., Singh, M. K., & Sousa, C. M. (2020). *of*. https://doi.org/10.1016/j.ref.2020.06.004

[39] Sundar, L. S., Singh, M. K., Punnaiah, V., & Sousa, A. C. M. (2017). Experimental investigation of Al2O3/water nanofluids on the effectiveness of solar flat-plate collectors with and without twisted tape inserts. *Renewable Energy*. https://doi.org/10.1016/j.renene.2017.10.056

[40] Vahidinia, F., & Khorasanizadeh, H. (2021). Development of new algebraic derivations to analyze minichannel solar fl at plate collectors with small and large size minichannels and performance evaluation study. *Energy*, *228*, 120640. https://doi.org/10.1016/j.energy.2021.120640

[41] Zayed, M. E., Zhao, J., Du, Y., Kabeel, A. E., & Shalaby, S. M. (2019). Factors a ff ecting the thermal performance of the fl at plate solar collector using nano fl uids : A review. *Solar Energy*, *182*(November 2018), 382–396. https://doi.org/10.1016/j.solener.2019.02.054